

Simulations and Experimental Demonstration of Coupling Molecular and Macroscopic Level Modalities with a Robotic Manipulator

Ahmet E. Sonmez, *Member, IEEE*, Yousef Hedayati, *Member, IEEE*, Alpay Özcan, *Senior Member, IEEE*, William M. Spees, Nikolaos V. Tsekos, *Member, IEEE*

Abstract— Established and emerging molecular and cellular modalities, such as optical imaging and spectroscopy, offer new opportunities for assessing tissue pathophysiology *in situ*. A challenge with such applications is their limited tissue penetration and low sensitivity that can be addressed with trans-needle or trans-catheter access. In this work, we describe the use of an actuated manipulator to physically manipulate such sensors to scan an area of interest generating 1-D scans while registering them to a guiding modality. Simulations were performed for a miniature RF coil to determine the voxel size, and experimental studies were conducted using a miniature RF coil manipulated by the MR-compatible device. The experimental results on phantom studies show that potential diagnostic information can be collected by using this methodology. This system was pursued to address a critical limitation of emerging molecular and near-cellular modalities; the limited tissue penetration.

I. INTRODUCTION

MOLECULAR and near-cellular imaging as well as the spectroscopy modalities offer new opportunities in biology and clinical medicine. Concurrent emergence of such advanced imaging and spectroscopy modalities open new windows for solving basic biological problems as in metabolic physiology, neuroscience, developmental biology; furthermore those modalities may facilitate clinical diagnosis such as assessing the malignancy of a tumor *in situ* (e.g., [1, 2]).

In several clinical paradigms, multimodality approaches are more appropriate for the collection of complementary diagnostic information (e.g., in the case of breast cancer [3-5]). However, molecular and cellular level modalities, such as optical coherence tomography (OCT) and light induced fluorescence (LIF) [6], have limited tissue penetration (~ 2 millimeters (mm)). Likewise due to the inherent low

sensitivity of the magnetic resonance imaging (MRI) and spectroscopy (MRS) many scientific studies cannot be performed [7].

Trans-catheter and trans-needle approaches have been introduced to address the low penetration or sensitivity of those “Limited field-of-view (Lim-FOV)” modalities by physically locating the sensor at close proximity to or inside of the anatomic locus of interest. For example, in the field of MR this practice has been adopted to address the inherent low sensitivity of MRI and MRS, by using radiofrequency (RF) coils that have been miniaturized for intra-vascular [8], intra-rectal [9] and intra-urethral [10] access.

Using miniaturized sensors for Lim-FOV creates a plethora of new imaging techniques with inherent benefits. One such benefit, for instance, lies in the field of MR where the maximum sensitivity can be enhanced by making the coil as small as possible. [11, 12]. However, in order to examine a large area of tissue with a miniature sensor, the sensor must be physically repositioned, thus a conventional imaging technique with higher tissue penetration must be used to guide the placement of the Lim-FOV sensor; such modalities can be MRI or ultrasound [2]. We will refer to the guiding imaging modalities as the “Wide-FOV” modalities.

The ability to combine modalities that interrogate the tissue at different levels (i.e., molecular, cellular and macroscopic) is a breakthrough in biology and clinical medicine. In this paper we demonstrate and implement a methodology in a phantom study that enables Lim-FOV imaging under the guidance of a Wide-FOV modality. Simulations are performed for determining the shape and size of the voxel of miniature RF coil sensing. Then by using the same miniature RF coil, a proof-of-concept work is demonstrated with the phantom studies, that are performed under the guidance of MRI (refers to the Wide-FOV modality). MRS is performed by miniature RF coil (refers to the Lim-FOV modality) for both RF transmission and signal reception, and MRS data was collected from a predefined trajectory inside of an access cannula.

II. METHODS

A. Overview of the Approach

In this work, we propose an approach which is based on a computer-controlled and actuated mechanical coupling between different modalities. We propose to use an actuated

Manuscript received April 15, 2010. This work was supported by the National Science Foundation (NSF) award CNS-0932272. All opinions, findings, conclusions or recommendations expressed in this work are those of the authors and do not necessarily reflect the views of our sponsors.

Nikolaos V. Tsekos is with the Medical Robotics Laboratory, Department of Computer Science at University of Houston, Houston, TX 77204 USA (phone: 713-743-3350; fax: 713-743-3335; e-mail: ntsekos@cs.uh.edu).

Ahmet E. Sonmez and Yousef Hedayati with the Medical Robotics Laboratory, Department of Computer Science at University of Houston, Houston, TX 77204 USA (e-mail: asonmez@uh.edu, yshedayati@uh.edu).

Alpay Ozcan and William M. Spees are with the Biomedical Magnetic Resonance Laboratory, Washington University, St. Louis, MO, USA (e-mail: ozcan@zach.wustl.edu, spees@wuchem.wustl.edu)

manipulator that carries a Lim-FOV sensor array, delivers it locally to the targeted tissue via a trans-cannula approach and spatially scans by mechanically relocating the array[13]. This generates one dimensional scans (herein referred to as “1-D scans”). The operational principle of this is specifically:

--A robotic manipulator is used to carry and mechanically scan an area of interest with one or multiple Lim-FOV sensor(s) (Fig. 1(a)). For *in vivo* applications, the sensors are deployed via trans-needle access. The scanning resolution can be determined pre-experimentally by evaluating the Lim-FOV specific voxel sizes, according to simulation results (Fig. 1(b)).

--A Wide-FOV macroscopic level imaging modality is incorporated to the multimodality data collection protocol in order to: (a) image the tissue at the macroscopic level, and (b) identify the targeted area where the manipulator mechanically scans with the Lim-FOV sensor. MRI offers the benefit of an inherent coordinate system.

--A registration protocol is utilized to register the manipulator relative to the Wide-FOV modality, and an encoder attached to the manipulator is used to maintain registration as the manipulator traverses the areas where the 1DScans are collected.

Based on the above registration of the manipulator and the Lim-FOV sensor(s), the Lim-FOV scans are co-registered to the Wide FOV images. In this proof-of-concept work we evaluated this approach first with experiments and then multimodal feasibility is evaluated via simulations.

B. Simulations

To investigate the proposed approach we first performed simulations to assess the spatial sensitivity profile of our Lim-FOV sensor: the miniature RF coil. Mapping of those profiles is useful for (a) determining the characteristics of the Lim-FOV sensors, and thus selecting their specifications (e.g., size of RF coil and aperture of the optical fibers for LIF) and (b) determining the shape and size of the voxel for each Lim-FOV modality pre-experimentally.

To find the RF coil reception profile, a simulation program was developed within the MATLAB environment that utilizes the Biot-Savart law. The software is capable of importing a .stl file that contains the vertex and face data of a coil designed in 3D CAD software. Once the coil data is

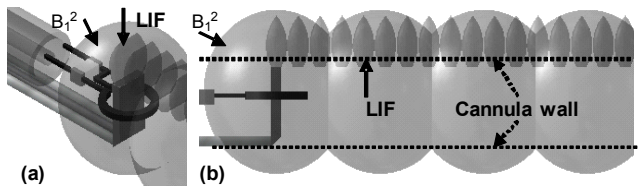


Fig. 1 Illustration of the dual Lim-FOV scanning. (a) multiple sensors can be attached to the distal end of the manipulator (b) Blobs delineating the Lim-FOV voxels are generated by 3D simulations. Then the voxels are superimposed to the LIF+MRS probe. Streaming-like collection of LIF interleaved to MRS.

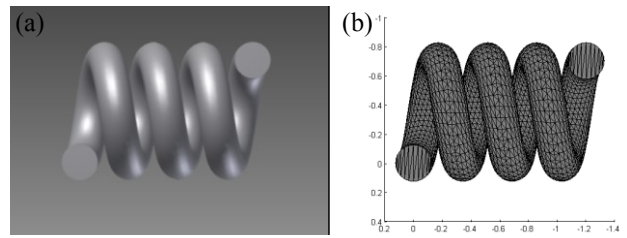


Fig. 2 (a) 3-D CAD drawing of coil (b) coil shape imported to the in house developed MATLAB code.

loaded a matrix is then defined to represent the virtual volume surrounding the coil. The Biot-Savart law is then applied to every point within that virtual space to determine the magnetic field created by the coil. Fig 2(a) shows the CAD drawing of our coil which is a 3.5 turn solenoid coil with outer diameter of 1.1 mm and height of 1.2 mm, and Fig 2(b) shows the coil imported to our software.

C. System

The manipulator was physically prototyped using a 3-D Fused Deposition Modeling printer (Prodigy Plus model, Stratasys, Eden Prairie, MN) out of non-magnetic and non-conductive acrylonitrile butadiene styrene (ABS) (Fig. 3(a)). Actuation was performed with a Squiggle motor (New Scale Technologies Inc., Victor, NY) connected via a 6 meter (m) length of shielded cable to the motor control unit. In-house made quadrature encoder and end stop switches were used for closed-loop control. A 3.5 turn miniature solenoid RF coil was made with a diameter of 1.1-mm and length of 1.2 mm (Fig. 3(c)) tuned to the proton Larmor frequency of 201.5 MHz for operation with the employed Varian DirectDrive 4.7 Tesla and 21 cm bore MRI scanner (Varian NMR, Palo Alto, CA) spectrometer/imager system. The miniature RF coil was attached to the distal end of the manipulator (Fig. 2(a)).

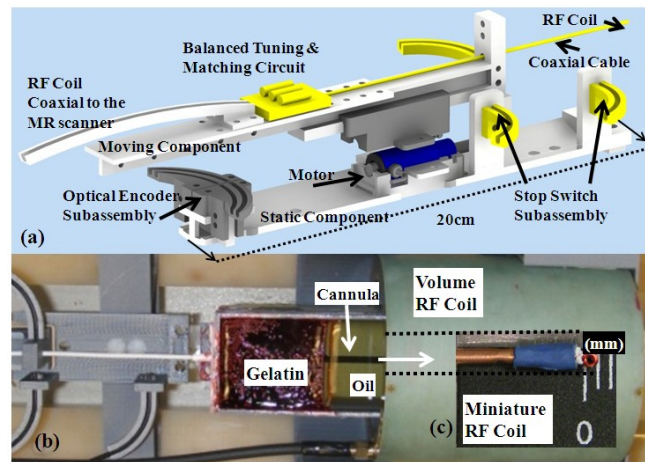


Fig. 3 (a) 3D design of the robotic manipulator (b) Experimental set up and (c) miniature RF coil.

The manipulator was controlled by a PC via a serial port to the motor controller (MC-1000, New Scale Technologies Inc., Victor, NY). To collect the MRS automatically a digital input/output unit (DI-148U, DATAQ Instruments Inc, Akron, OH) was used as the triggering unit, which was synchronously interfaced to the MR console to trigger the MRS for collection, and the manipulator for actuation.

To co-register MR images and MR spectra using the mechanical coupling provided by the robotic manipulator we used the inherent coordinate system of the MR scanner. Using this approach makes the system versatile and robust for using other types of Lim-FOV modalities for co-registered scanning. To achieve this co-registration we first used a miniature RF coil as a fiducial marker [14-16]. Then the transient position of the Lim-FOV sensor array is thereafter determined from the quadrature linear optical encoder.

D. Experiments

The system was tested with experimental studies using a two-compartment phantom, one compartment was filled with gelatin and the other with vegetable oil (Fig. 3(b)). With the manipulator in place, the phantom was placed inside a volume RF coil to collect scout images. By using the scout images the device was registered to the MR scanner. An in-house developed graphical user interface (GUI) allowed the operator to decide the scanning protocol (region, steps and speed of motion). 1-D scan MRS data was collected by translating the miniature RF coil in steps of 1.0 mm. After a translation step, the control module triggered the MR spectrometer with a TTL pulse to collect the free induction decay (FID) after a single excitation pulse (with a flip angle = 45°, bandwidth = 5000 Hz and number of points = 2048). Upon completion of each data set collection, the MR scanner triggered the control module to advance the sensor to the next position.

III. RESULTS AND DISCUSSION

Fig. 4(a) shows the MR image collected by the miniature RF coil from the sagittal plane (center of the coil in y-z plane of the MR scanner). Fig. 4(b) is the simulation result of the virtual coil showing the rotating magnetic field (B_1) profile of a four-turn solenoid coil with the dimensions of the one used in the experimental studies through the same plane as seen in Fig. 4(a). The RF coil reception profile determines the shape and size of the voxel of the MRS sensor. Determining the characteristics of the Lim-FOV sensors can help to select required coil specifications (e.g., size of RF coil or aperture of the optical fibers for LIF). Moreover, determining the shape and size of the voxel for each Lim-FOV modality pre-experimentally can help plan the spacing for the MRS 1-D scans.

Fig. 5 shows results from a representative 30 mm long, 1-mm resolution 1-D scan acquisition along the axis of the cannula on the two-compartment phantom (zoomed MRI to the scanning region). Fig. 5(a) and 5(b) are sample spectra

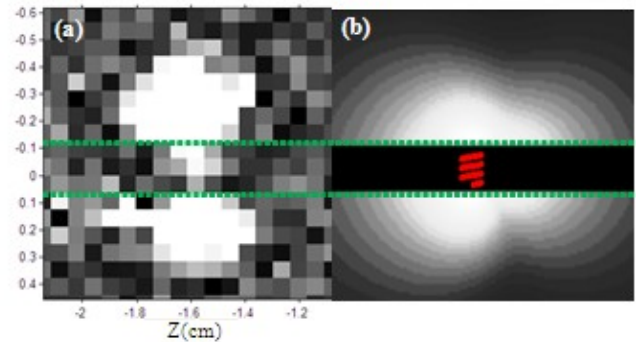


Fig. 4 (a) MR image collected by the miniature RF coil from the sagittal plane of the coil. No signal area in the MR image between the two dashed lines delineates the cannula that the miniature RF coil was traversing in. (b) Results from the simulation showing the excitation profile of the miniature RF coil for side by side comparison.

collected with the miniature RF coil respectively from the gelatin compartment and the oil compartment. Fig. 5(c) shows the integrated intensity of a spectral band (spectral band delineated with a cap on figures 5(a) and 5(b)) belonging to the oil resonance, co-registered and overlapped on to the MRI image. The transition from the gelatin filled compartment to the one with vegetable oil is apparent at $Z=0.2$ cm. This is manifested with the emergence of the signals originating from the oil compartment.

It is noted that the assignment of the Z coordinates was based on the initial registration of the device. Then by using the recorded encoder values, the current position is calculated, and saved into the log-file.

This work describes an approach that uses a mechanical manipulator to generate 1-D spatial distribution of the sensor data (i.e., a 1-D scan). Using standard robotic methodology, the spatially localized Lim-FOV sensor data are registered relative to the guiding Wide-FOV modality.

Due to the limited tissue penetration of the Lim-FOV sensors, a trans-needle access was used. Such minimally

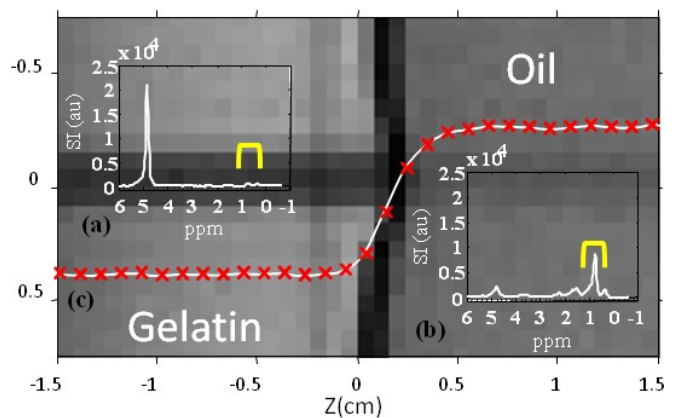


Fig. 5 (a) and (b) are sample spectra collected from gelatin and vegetable oil compartments respectively with miniature RF coil (b) Integrated intensity (given unitless to illustrate relative change) of spectral band delineated with a cap on (a) and (b). On (c) each cross refers to a spectra collected from corresponding Z axis value of MR scanner.

invasive diagnostic approaches are commonly practiced, including biopsies and optical imaging. In clinical applications, the merit of minimally invasive approaches is evaluated within the context of the potential diagnostic information that can be collected. As an example, the particular sensor presented herein, i.e., a miniature RF coil for MR spectroscopy can be beneficial for spectroscopy in lower magnetic field scanners where the proximity of the coil would improve the inherent sensitivity of the modality (e.g., in the case of combining MRI and MRS in breast cancer assessment [17].)

This proof-of-concept work has certain limitations. First, studies were only performed on phantoms; *in vitro* and *in vivo* studies are planned. Second, the proposed approach was demonstrated experimentally using proton MRS as the only Lim-FOV modality. Currently we are developing a LIF probe based on optical fibers for excitation and reception and we will combine it with the miniature RF coil. This implementation will allow the experimental evaluation and *in vivo* application of the multimodality system. It should be emphasized that the system was designed as an enabling-technology platform that can be adopted to carry and perform scanning with other types of sensors, such as endoscopic OCT or LIF.

IV. CONCLUSION

This work describes a novel application for biology and medicine to facilitate multimodality imaging by carrying, scanning and co-registering localized bio-sensing. This specific application of robotics was pursued to address a critical limitation of emerging molecular and near-cellular modalities; the limited tissue penetration. In this proof-of-concept work, the approach is first evaluated with simulations and then experimentally demonstrated with a miniature RF coil for collecting MRS on two compartment phantoms. The described system is under further development for the incorporation of a range of miniature biosensors.

REFERENCES

[1] D. J. Margolis, J. M. Hoffman, R. J. Herfkens, R. B. Jeffrey, A. Quon, and S. S. Gambhir, "Molecular imaging techniques in body imaging," *Radiology*, vol. 245, pp. 333-56, Nov 2007.

[2] Q. Zhu, M. Huang, N. Chen, K. Zarfos, B. Jagjivan, M. Kane, P. Hedge, and S. H. Kurtzman, "Ultrasound-guided optical tomographic imaging of malignant and benign breast lesions: initial clinical results of 19 cases," *Neoplasia*, vol. 5, pp. 379-88, Sep-Oct 2003.

[3] S. E. Harms and D. P. Flamig, "Breast MRI," *Clin Imaging*, vol. 25, pp. 227-46., 2001.

[4] A. P. Smith, P. A. Hall, and D. M. Marcello, "Emerging technologies in breast cancer detection," *Radiol Manage*, vol. 26, pp. 16-24; quiz 25-7, Jul-Aug 2004.

[5] C. P. Behrenbruch, K. Marias, P. A. Armitage, M. Yam, N. Moore, R. E. English, J. Clarke, and M. Brady, "Fusion of contrast-enhanced breast MR and mammographic imaging data," *Med Image Anal*, vol. 7, pp. 311-40, Sep 2003.

[6] F. A. Jaffer, C. Vinegoni, M. C. John, E. Aikawa, H. K. Gold, A. V. Finn, V. Ntziachristos, P. Libby, and R. Weissleder, "Real-time catheter molecular sensing of inflammation in proteolytically active atherosclerosis," *Circulation*, vol. 118, pp. 1802-9, Oct 28 2008.

[7] A. G. Webb, "Microcoil nuclear magnetic resonance spectroscopy," *Journal of Pharmaceutical and Biomedical Analysis*, vol. 38, pp. 892-903, Aug 10 2005.

[8] B. Qiu, F. Gao, P. Karmarkar, E. Atalar, and X. Yang, "Intracoronary MR imaging using a 0.014-inch MR imaging-guidewire: toward MRI-guided coronary interventions," *J Magn Reson Imaging*, vol. 28, pp. 515-8, Aug 2008.

[9] R. C. Susil, C. Menard, A. Krieger, J. A. Coleman, K. Camphausen, P. Choyke, G. Fichtinger, L. L. Whitcomb, C. N. Coleman, and E. Atalar, "Transrectal prostate biopsy and fiducial marker placement in a standard 1.5T magnetic resonance imaging scanner," *J Urol*, vol. 175, pp. 113-20, Jan 2006.

[10] H. H. Quick, J. M. Serfaty, H. K. Pannu, R. Genadry, C. J. Yeung, and E. Atalar, "Endourethral MRI," *Magn Reson Med*, vol. 45, pp. 138-46, Jan 2001.

[11] D. I. Hoult and R. E. Richards, "Signal-to-Noise Ratio of Nuclear Magnetic-Resonance Experiment," *Journal of Magnetic Resonance*, vol. 24, pp. 71-85, 1976.

[12] T. L. Peck, R. L. Magin, and P. C. Lauterbur, "Design and Analysis of Microcoils for Nmr Microscopy," *Journal of Magnetic Resonance Series B*, vol. 108, pp. 114-124, Aug 1995.

[13] A. E. Sonmez, A. Özcan, W. M. Spees, and N. V. Tsekos, "Robot-facilitated Scanning and Co-registration of Multi-modal and Multi-level Sensing: Demonstration with Magnetic Resonance Imaging and Spectroscopy," in *Proceedings of IEEE International Conference on Robotics and Automation*, Shanghai, China, 2011, pp. 1113-1138.

[14] G. A. Coutts, D. J. Gilderdale, M. Chui, L. Kasuboski, and N. M. DeSouza, "Integrated and interactive position tracking and imaging of interventional tools and internal devices using small fiducial receiver coils," *Magn Reson Med*, vol. 40, pp. 908-13, Dec 1998.

[15] C. Flask, D. Elgort, E. Wong, A. Shankaranarayanan, J. Lewin, M. Wendt, and J. L. Duerk, "A method for fast 3D tracking using tuned fiducial markers and a limited projection reconstruction FISP (LPR-FISP) sequence," *J Magn Reson Imaging*, vol. 14, pp. 617-27, Nov 2001.

[16] K. Shimizu, R. V. Mulkern, K. Oshio, L. P. Panych, S. S. Yoo, R. Kikinis, and F. A. Jolesz, "Rapid tip tracking with MRI by a limited projection reconstruction technique," *J Magn Reson Imaging*, vol. 8, pp. 262-4, Jan-Feb 1998.

[17] P. J. Bolan, M. T. Nelson, D. Yee, and M. Garwood, "Imaging in breast cancer: Magnetic resonance spectroscopy," *Breast Cancer Res*, vol. 7, pp. 149-52, 2005.